



A new statistical model for plasmaspheric hiss and its effect on electron losses

T. Kersten, R. B. Horne, N. P. Meredith, S. A. Glauert (1)

(1) *British Antarctic Survey, UK*

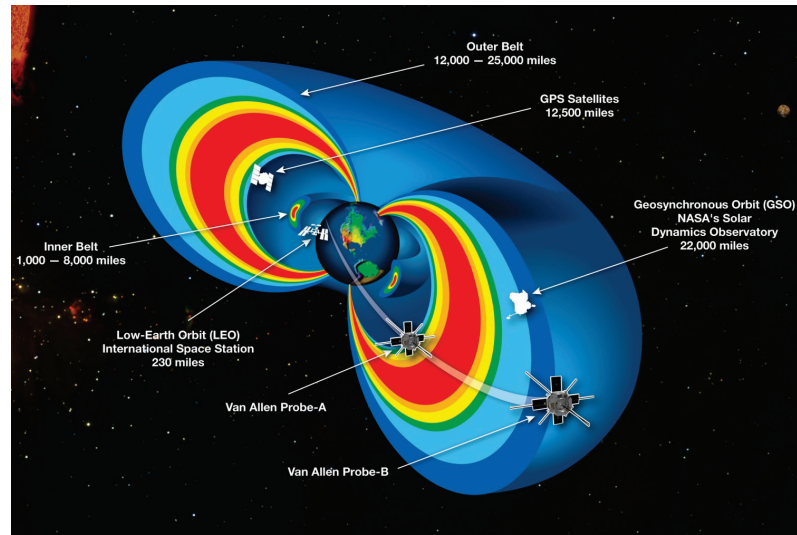
The research leading to these results funded in part by the European Union Seventh Framework Programme (FP7) under grant agreement No 606716 SPACESTORM

Lunar MIST, Lancaster, UK, 05/04/2016 – 07/04/2016



Van Allen Radiation Belts

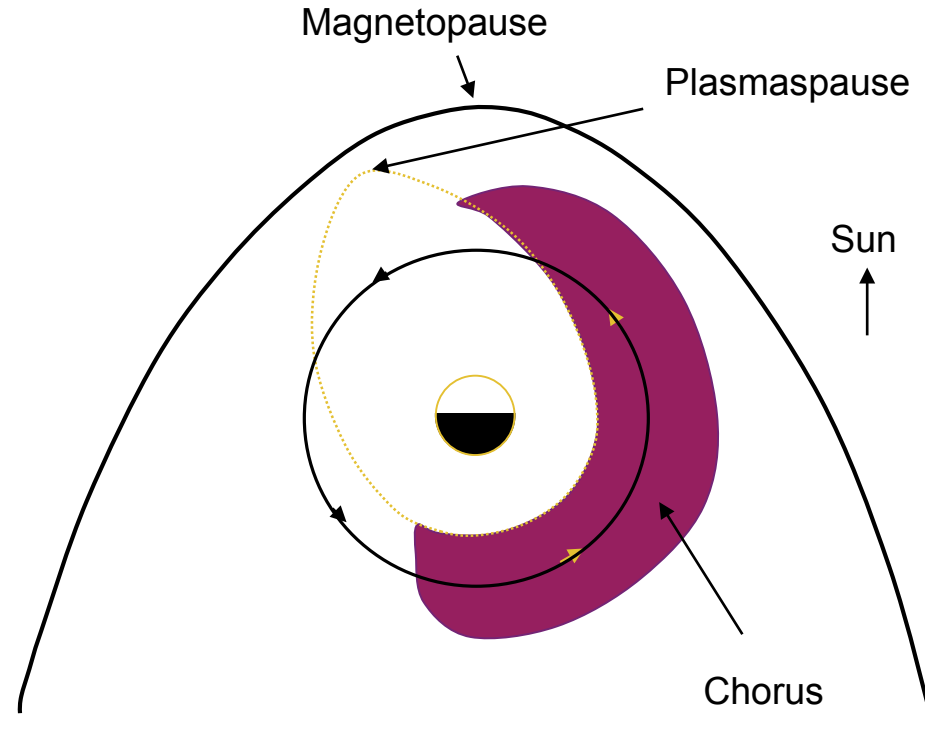
- Risk for spacecraft
- Danger for humans in space
- Inner belt: stable
- Outer belt: highly variable
- Main cause for variability:
Plasma waves



Source: NASA

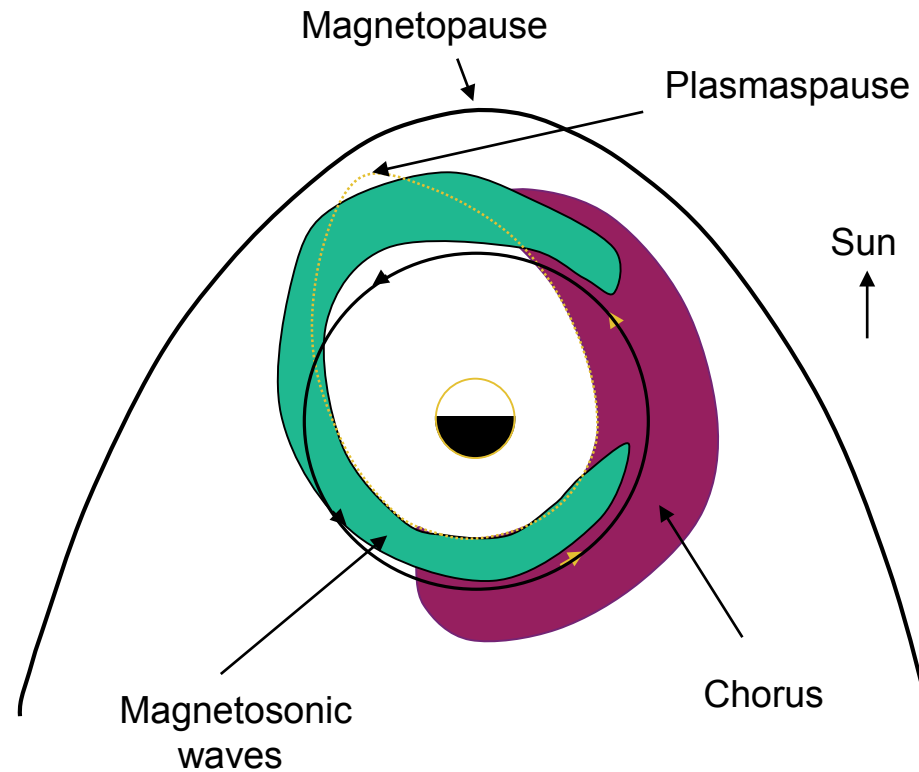
Types of plasma waves

- *Chorus waves:*
 - Major cause of acceleration and loss



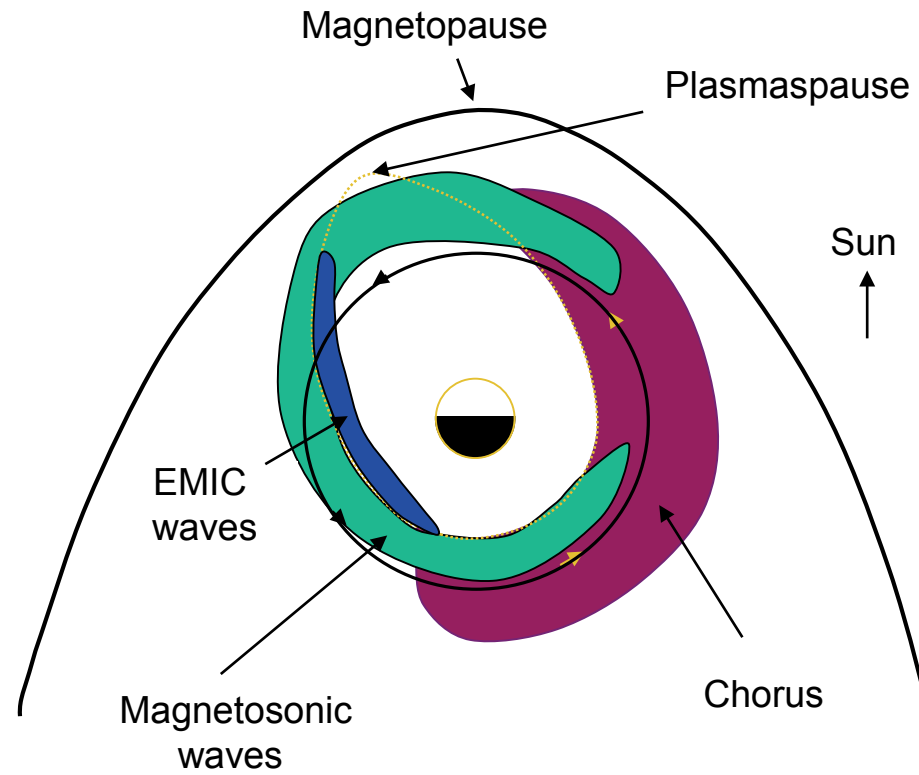
Types of plasma waves

- *Chorus waves*:
 - Major cause of acceleration and loss
- *Magnetosonic waves*:
 - May be an important acceleration mechanism



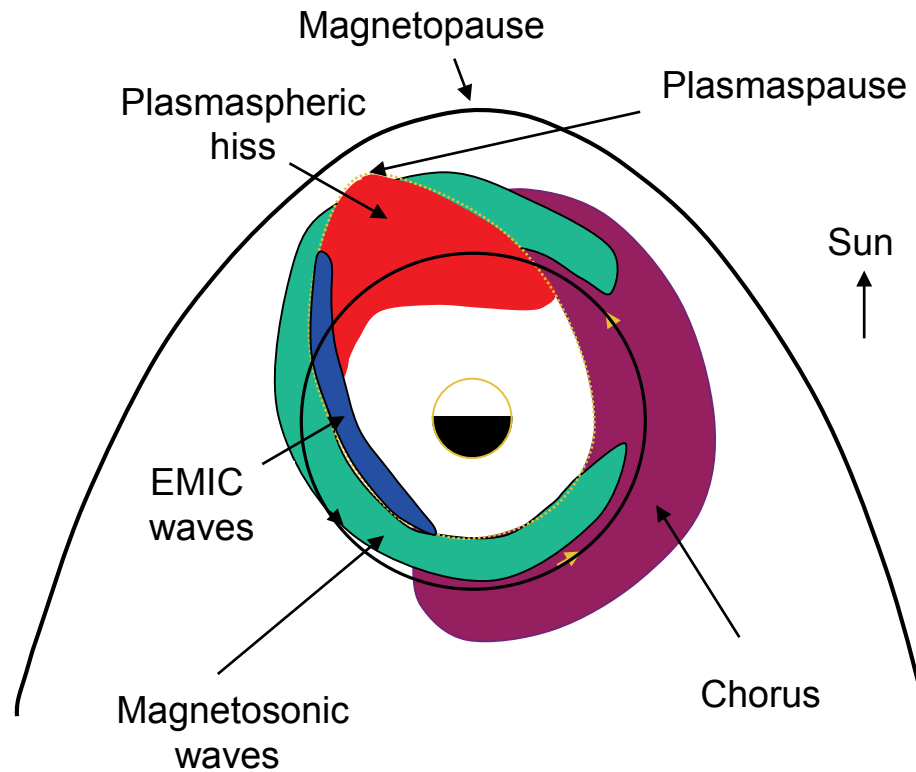
Types of plasma waves

- *Chorus waves*:
 - Major cause of acceleration and loss
- *Magnetosonic waves*:
 - May be an important acceleration mechanism
- *EMIC waves*:
 - Losses of ultrarelativistic electrons at low pitch-angles



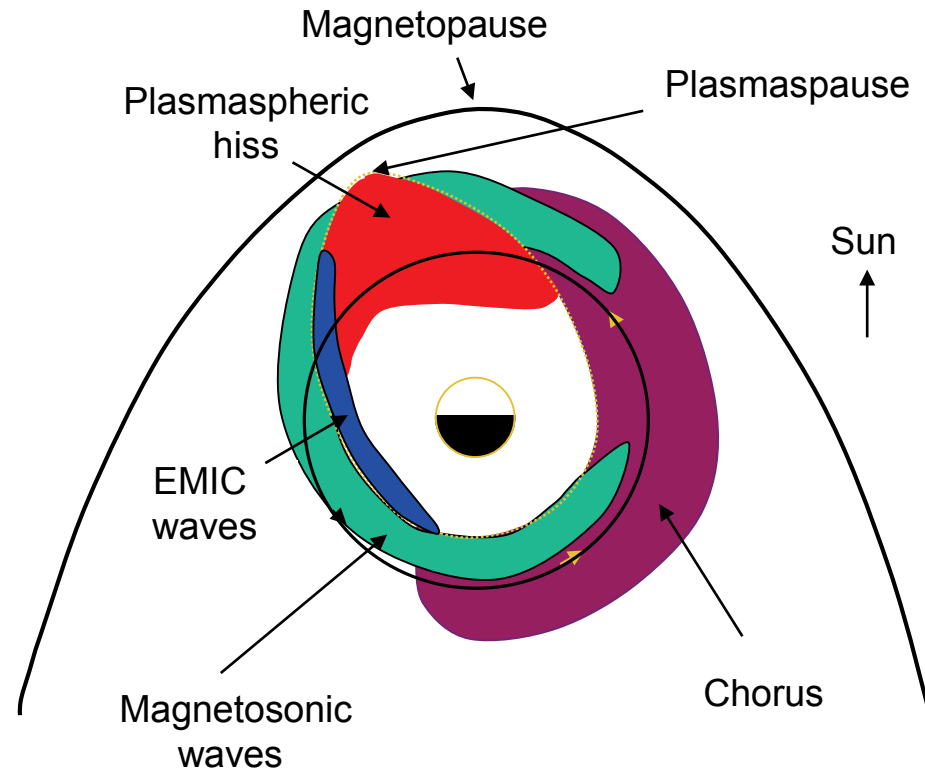
Types of plasma waves

- *Chorus waves*:
 - Major cause of acceleration and loss
- *Magnetosonic waves*:
 - May be an important acceleration mechanism
- *EMIC waves*:
 - Losses of ultrarelativistic electrons at low pitch-angles
- *Plasmaspheric hiss*:
 - Major loss process



Types of plasma waves

- *Chorus waves*:
 - Major cause of acceleration and loss
- *Magnetosonic waves*:
 - May be an important acceleration mechanism
- *EMIC waves*:
 - Losses of ultrarelativistic electrons at low pitch-angles
- *Plasmaspheric hiss*:
 - Major loss process



Objective of Study: Determine the effectiveness of hiss

Modelling the Radiation Belts

BAS Radiation Belt Model

- Fokker-Planck Equation

$$\frac{\partial f}{\partial t} = L^2 \frac{\partial}{\partial L} \left(\frac{D_{LL}}{L^2} \frac{\partial f}{\partial L} \right)_{\mu J} + \frac{1}{g(\alpha)} \frac{\partial}{\partial \alpha} \left(g(\alpha) D_{\alpha\alpha} \frac{\partial f}{\partial \alpha} \right)_{EL} + \frac{1}{A(E)} \frac{\partial}{\partial E} \left(A(E) D_{EE} \frac{\partial f}{\partial E} \right)_{\alpha L} - \frac{f}{\tau(\alpha, E)}$$

BAS Radiation Belt Model

- Fokker-Planck Equation

$$\frac{\partial f}{\partial t} = L^2 \frac{\partial}{\partial L} \left(\frac{D_{LL}}{L^2} \frac{\partial f}{\partial L} \right) \Big|_{\mu L} + \frac{1}{g(\alpha)} \frac{\partial}{\partial \alpha} \left(g(\alpha) D_{\alpha\alpha} \frac{\partial f}{\partial \alpha} \right) \Big|_{EL} + \frac{1}{A(E)} \frac{\partial}{\partial E} \left(A(E) D_{EE} \frac{\partial f}{\partial E} \right) \Big|_{\alpha L} - \frac{f}{\tau(\alpha, E)}$$

Radial transport

BAS Radiation Belt Model

- Fokker-Planck Equation

$$\frac{\partial f}{\partial t} = L^2 \frac{\partial}{\partial L} \left(\frac{D_{LL}}{L^2} \frac{\partial f}{\partial L} \right)_{\mu L} + \frac{1}{g(\alpha)} \frac{\partial}{\partial \alpha} \left(g(\alpha) D_{\alpha\alpha} \frac{\partial f}{\partial \alpha} \right)_{EL} + \frac{1}{A(E)} \frac{\partial}{\partial E} \left(A(E) D_{EE} \frac{\partial f}{\partial E} \right)_{\alpha L} - \frac{f}{\tau(\alpha, E)}$$

Radial transport

Pitch angle diffusion

BAS Radiation Belt Model

- Fokker-Planck Equation

$$\frac{\partial f}{\partial t} = L^2 \frac{\partial}{\partial L} \left(\frac{D_{LL}}{L^2} \frac{\partial f}{\partial L} \right)_{\mu L} + \frac{1}{g(\alpha)} \frac{\partial}{\partial \alpha} \left(g(\alpha) D_{\alpha\alpha} \frac{\partial f}{\partial \alpha} \right)_{EL} + \frac{1}{A(E)} \frac{\partial}{\partial E} \left(A(E) D_{EE} \frac{\partial f}{\partial E} \right)_{\alpha L} - \frac{f}{\tau(\alpha, E)}$$

Radial transport

Pitch angle diffusion

Energy diffusion

BAS Radiation Belt Model

- Fokker-Planck Equation

$$\frac{\partial f}{\partial t} = L^2 \frac{\partial}{\partial L} \left(\frac{D_{LL}}{L^2} \frac{\partial f}{\partial L} \right)_{\mu L} + \frac{1}{g(\alpha)} \frac{\partial}{\partial \alpha} \left(g(\alpha) D_{\alpha\alpha} \frac{\partial f}{\partial \alpha} \right)_{EL} + \frac{1}{A(E)} \frac{\partial}{\partial E} \left(A(E) D_{EE} \frac{\partial f}{\partial E} \right)_{\alpha L} - \frac{f}{\tau(\alpha, E)}$$

Radial transport Pitch angle diffusion Energy diffusion Losses

BAS Radiation Belt Model

- Fokker-Planck Equation

$$\frac{\partial f}{\partial t} = L^2 \frac{\partial}{\partial L} \left(\frac{D_{LL}}{L^2} \frac{\partial f}{\partial L} \right)_{\mu L} + \frac{1}{g(\alpha)} \frac{\partial}{\partial \alpha} \left(g(\alpha) D_{\alpha\alpha} \frac{\partial f}{\partial \alpha} \right)_{EL} + \frac{1}{A(E)} \frac{\partial}{\partial E} \left(A(E) D_{EE} \frac{\partial f}{\partial E} \right)_{\alpha L} - \frac{f}{\tau(\alpha, E)}$$

Radial transport Pitch angle diffusion Energy diffusion Losses

- Drift & bounce averaged diffusion coefficients D_{LL} , $D_{\alpha\alpha}$, D_{EE} are activity, location and energy dependent

BAS Radiation Belt Model

- Fokker-Planck Equation

$$\frac{\partial f}{\partial t} = L^2 \frac{\partial}{\partial L} \left(\frac{D_{LL}}{L^2} \frac{\partial f}{\partial L} \right)_{\mu L} + \frac{1}{g(\alpha)} \frac{\partial}{\partial \alpha} \left(g(\alpha) D_{\alpha\alpha} \frac{\partial f}{\partial \alpha} \right)_{EL} + \frac{1}{A(E)} \frac{\partial}{\partial E} \left(A(E) D_{EE} \frac{\partial f}{\partial E} \right)_{\alpha L} - \frac{f}{\tau(\alpha, E)}$$

Radial transport Pitch angle diffusion Energy diffusion Losses

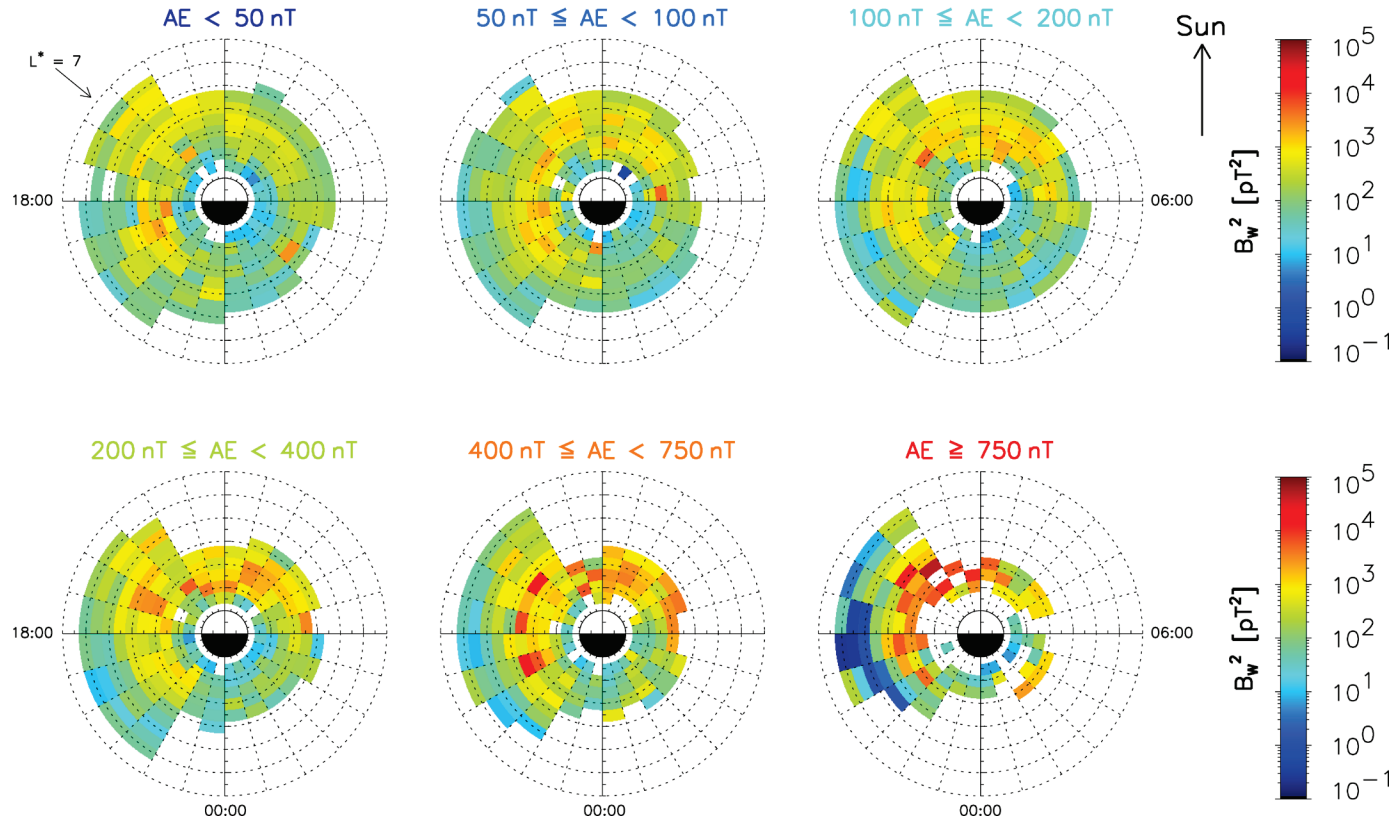
- Drift & bounce averaged diffusion coefficients D_{LL} , $D_{\alpha\alpha}$, D_{EE} are activity, location and energy dependent
- Calculate $D_{\alpha\alpha}$ and D_{EE} with PADIE diffusion code [Glauert and Horne, 2005]
- Requires wave spectral data -> Wave model

New Plasmaspheric Hiss Model

- Wave spectral data from seven different satellites:
CRRES, Double Star TC1, Dynamics Explorer 1, Cluster 1,
THEMIS A, D, and E
- Derived statistical model for plasmaspheric hiss:
 - Frequency range covered: 100 Hz – 4 kHz
 - 12 levels of L^* covering $1.5 < L^* < 7.0$ (in steps of $0.5 L^*$)
Includes hiss in plumes
 - 24 levels of MLT
 - 10 levels of geomagnetic latitude covering $3^\circ < \lambda_m < 60^\circ$ (in steps of 6°)
 - 6 levels of geomagnetic activity (AE)

Plasmaspheric Hiss – Wave Power

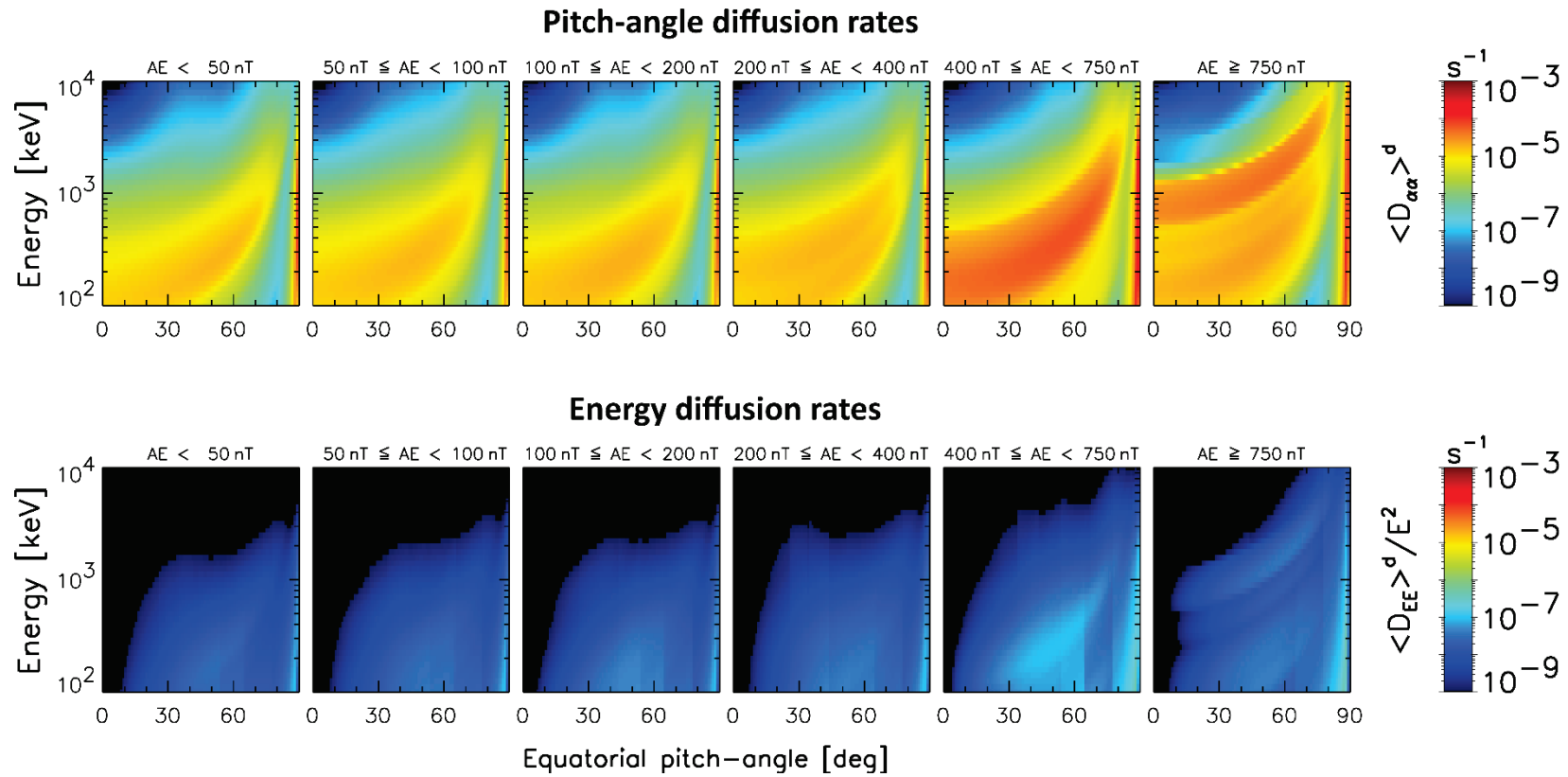
Integrated hiss wave power B_w^2 in the region $3^\circ < |\lambda_m| < 9^\circ$



Diffusion Rates

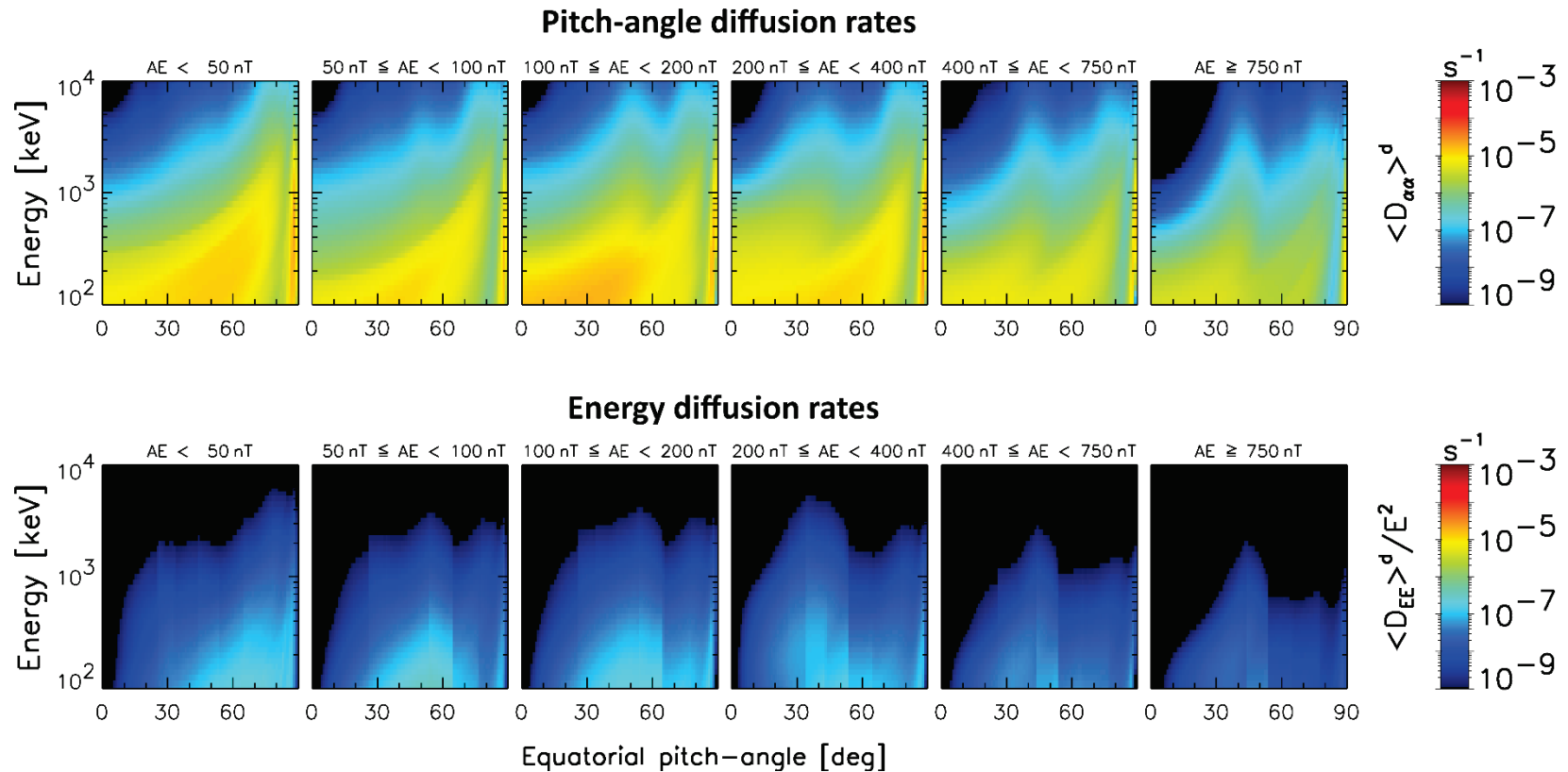
Drift and Bounce Averaged Diffusion Rates

Drift and bounce averaged diffusion rates - $L^* = 3.5$ $0^\circ < |\lambda_m| < 60^\circ$



Drift and Bounce Averaged Diffusion Rates

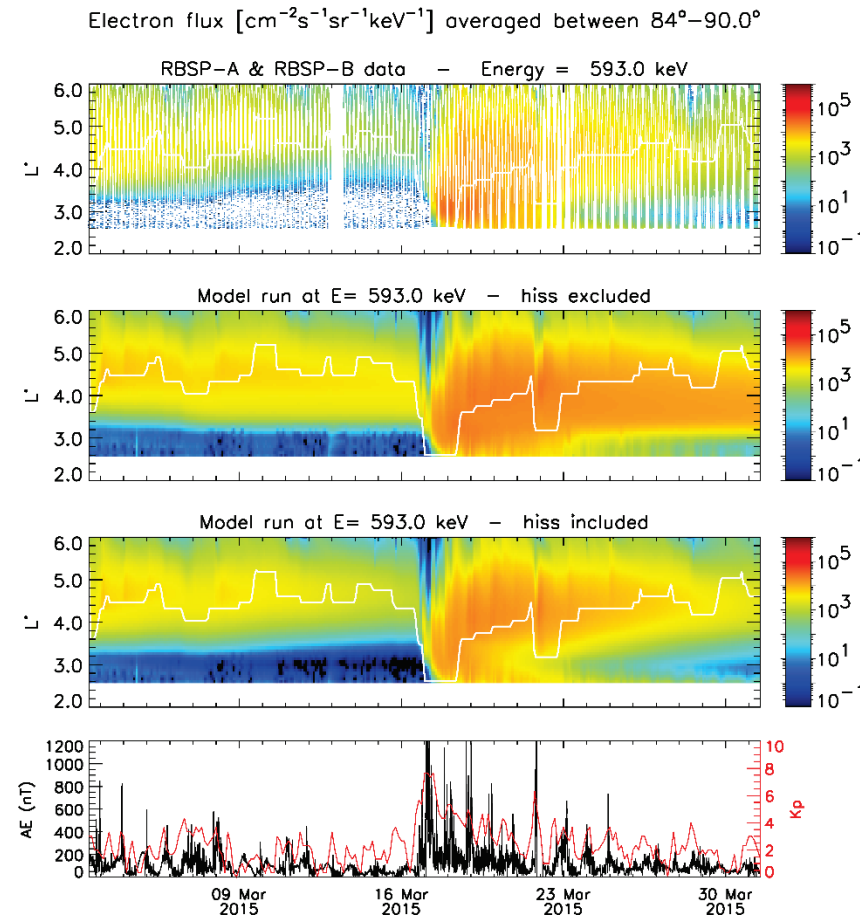
Drift and bounce averaged diffusion rates - $L^* = 5.5$ $0^\circ < |\lambda_m| < 60^\circ$



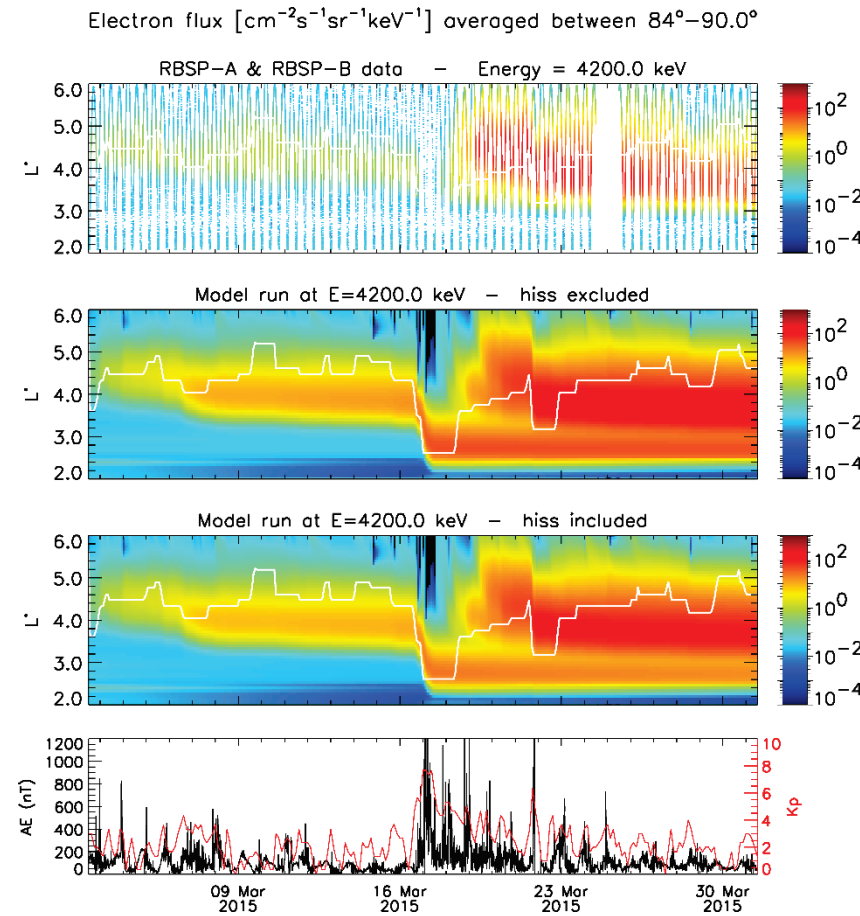
Electron Flux

- Selected Van Allen Probes period:
03 March 2015 – 31 March 2015 (St. Patrick's day storm)
- BAS RBM driven by:
 - Brautigam & Albert radial diffusion coefficients
 - Our most recent lower and upper band chorus wave model
 - Our most recent EMIC wave model
 - Presented plasmaspheric hiss wave model
- Initial and Boundary conditions derived from VAP data

90° Electron Flux – 593 keV

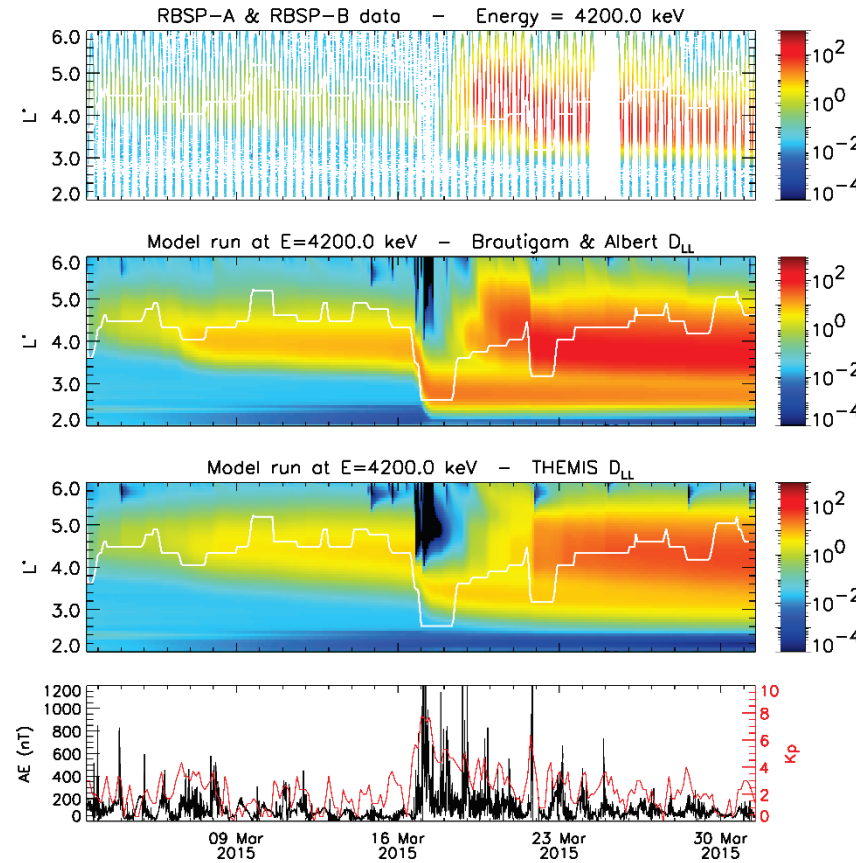


90° Electron Flux – 4200 keV



90° Electron Flux – 4200 keV – D_{LL} Comparison

Electron flux [$\text{cm}^{-2}\text{s}^{-1}\text{sr}^{-1}\text{keV}^{-1}$] averaged between 84°–90.0°



Summary and Conclusions

- Developed statistical hiss wave model based on data from 7 satellites.
- Considerably improved resolution of L^* , MLT, and geomagnetic activity
- Hiss provides good agreement with VAP data between 100 keV and 1 MeV
- There are issues for $E > 2$ MeV at low L^*
- Indications that radial diffusion too strong inside the plasmapause at high energies
- Is there evidence for reduced ULF wave power inside the plasmapause?

Acknowledgements

- The research leading to these results has received funding from the European Union Seventh Framework Programme under grant agreement number 606716 (SPACESTORM) and is also supported in part by the UK Natural Environment Research Council.